



A comparative study of critical pitting temperature (CPT) of stainless steels by electrochemical impedance spectroscopy (EIS), potentiodynamic and potentiostatic techniques

N. Ebrahimi, M. Momeni, A. Kosari, M. Zakeri, M.H. Moayed*

Metallurgical and Materials Engineering Department, Faculty of Engineering, Ferdowsi University of Mashhad, Mashhad 91775-1111, Iran

ARTICLE INFO

Article history:

Received 11 August 2011

Accepted 27 February 2012

Available online 9 March 2012

Keywords:

A. Stainless steel

B. EIS

B. Polarisation

B. Potentiostatic

C. Pitting corrosion

C. Passivity

ABSTRACT

In this study critical pitting temperature (CPT) of two stainless steels is compared using EIS, potentiodynamic and potentiostatic techniques. Two types of stainless steels including DSS2205 and 20Cr–28Ni were chosen. EIS measurements were carried at anodic potential of 600 mV/SCE and the results were compared with those of potentiodynamic and potentiostatic polarisations. The results revealed that the CPT of DSS2205 and 20Cr–28Ni was between 45–55 °C and 35–45 °C in potentiodynamic polarisation, respectively. It was 60 and 55 °C for potentiostatic method and between 55–60 °C and 45–55 °C in EIS method for DSS2205 and 20Cr–28Ni, respectively.

© 2012 Elsevier Ltd. All rights reserved.

1. Introduction

The critical pitting temperature (CPT) is an important characteristic of pitting which has been introduced from the early 1970s [1,2]. Production of high corrosion resistance stainless steels, which contain additional alloying elements (mainly Mo and N), introduced a wide range of stainless steels which no longer suffer from pitting at room temperature. Pitting corrosion tests on alloyed stainless steel at higher temperature revealed that their pitting is highly temperature dependent. The lowest temperature at which a stainless steel suffers from pitting corrosion is called the alloy CPT.

It was shown quantitatively that temperature is an important criterion for describing the onset of pitting corrosion in molybdenum-containing austenitic stainless steels in a series of pitting studies by Brigham and Tozer [1–5]. They compared the results of three independent test methods (two potentiostatically controlled and one freely corroding) in chloride solutions. Comparing the pitting temperature obtained with solutions of similar chloride activities but very different oxidising power, Brigham noted that there was not a strong dependence of the threshold temperature on potential. This suggests that there was a critical pitting temperature (CPT) below which the steel will not pit regardless of potential and exposure time. The potentiostatic method favoured by Brigham

involved applying an anodic potential of 500 mV (SCE) to test alloy in a 35% NaCl solution while its temperature was increased at rate of 0.6 °C/min. The temperature at which the current density increased sharply to a value of 100 $\mu\text{A}\cdot\text{cm}^{-2}$ (the criterion of pit initiation) was considered to be the temperature at which pitting began and was designated as the critical pitting temperature (CPT) [1].

The CPT of stainless steels can be determined using different procedures:

- A) By measuring potentiodynamic polarisation curves at different temperatures and plotting the breakdown potential vs. temperature, using special precautions (e.g., injection of distilled water) to prevent crevice corrosion. If the pitting test result is not affected by crevice corrosion, when variation of breakdown potential vs. temperature is plotted, CPT is the temperature where the breakdown potential falls down sharply from transpassive to pitting corrosion [6–8]. The pitting criterion used by Qvarfort [8] was the potential where the current density exceeded 100 $\mu\text{A}\cdot\text{cm}^{-2}$.
- B) The steel specimen is polarised at a fixed anodic potential, more noble than any possible breakdown potential, in an aggressive solution, the temperature of which is increased slowly (0.6 °C min^{-1}) and the CPT is the temperature at which a marked current increase is observed [9].
- C) According to the ASTM G 48 test, CPT can be also be determined by immersion of alloy samples in 10% FeCl_3 solution, the temperature is increased stepwise by 2.5 °C every 24 h.

* Corresponding author. Tel.: +98 5118763305; fax: +98 5118763301.

E-mail address: mhmoayed@um.ac.ir (M.H. Moayed).

The sample is then examined under an optical microscope to detect any pitting. The CPT is defined as the temperature below which no pits are observed [10].

- D) Determining the CPT by a Zero resistance ammeter (ZRA) technique. The coupled current flowing between the two connected identical electrodes, which are immersed in an oxidising solutions increases abruptly when pitting starts as the solution is heated up above the CPT [11,12].
- E) Determining the CPT by applying a weak galvanostatic anodic polarisation ($50\text{--}200\ \mu\text{A}\cdot\text{cm}^{-2}$) to a prepassivated (e.g., 5 min in 3 M nitric acid) alloy sample and recording the alloy potential while the electrolyte temperature is increased continuously. The CPT is defined at the sudden potential decrease due to stable pit formation [13,14]. In this case, the pitting incubation time and hence the CPT will be affected by the film characteristics of the prepassivated sample. An advantage of this method is that the initial potential, for resistant alloys, automatically lies at the beginning of the transpassive region [12].

2. Development of new method based on EIS technique

Several methods which are used for measuring CPT of high pitting resistance stainless steels focus on the changing of alloy behaviour from transpassivity to pitting corrosion in solution containing aggressive ions. As it was reported above, these measurement methods based on applied potential from the external source (e.g., a potentiostat) can be divided into two categories. Those which are performed at a constant temperature and the test are repeated in a certain steps of temperature. In the other category, at a single test running, the temperature is continuously raised and the temperature in which abrupt rising in current density was observed can be considered as the CPT value of alloy.

Electrochemical impedance spectroscopy (EIS) is now widely used to investigate the mechanisms and rates of corrosion. While its use is generally restricted to homogeneous corrosion situations in which, the whole sample surface undergoes the same processes, some attempts to extend impedance techniques to localised corrosion are reported in the recent literature [15–21]. However, the usefulness of EIS during localised corrosion depends on how much *ac* measurements improve the knowledge of the electrochemical processes in comparison to *dc* measurements. For pitting corrosion the question is to know whether or not EIS allows getting deeper understanding than *dc* current or potential variations. From *dc* variations the following parameters are not directly available: The change in the passive film properties and the rate determining process during pit growth [22].

From a rapid review of the literature, EIS seems to be able to investigate the stable pitting step more precisely, i.e. detection of pitting [15–17,19,20], estimation of the pitted fraction area [19] and the change in the chemical processes as a function of time [15]. Whereas, the change of the impedance during the pre-pitting step remains unclear [15].

To develop a new method for measuring CPT of alloys using the EIS, the measurements should be performed at potentials in which passivity is stable and it is sufficiently high for detection of changing the transpassivity mode to pitting corrosion. For example, in the ferric chloride solution test, this potential is produced by the changing of cathodic reaction from oxygen reduction to reduction of ferric (Fe^{3+}) to ferrous (Fe^{2+}) ions. In potentiostatic polarisation method, this potential is produced by applying an additional *dc* anodic potential. In this new method, *ac* measurements are performed at a high passive state potential by applying the additional *dc* potential, similar to that of potentiostatic method. In lower temperatures in which pitting corrosion does not occur, the EIS results contain only one semi circle which is related to the passive

surface. Further increase in temperature (similar to that of potentiodynamic polarisation method), changes the charge transfer resistance and capacitor of the double layer. When pitting corrosion occurs, the charge transfer resistance decreases significantly, because of the local activity of surface. In other word, since surface is locally activated and produces current which is significantly higher than that of passive surface [23], the charge transfer resistance decreases significantly. The lowest temperature in which this behaviour is observed can be considered as CPT.

In addition, since the surface is locally activated and the remained surface is in passive state, at lower frequencies an inductive loop can be detected. This inductive loop is observed because there are some sites in the surface which produce current [24–26]. An abrupt decrease in charge transfer resistance is sufficient to detect the CPT and this phenomenon can be found at high frequencies. To determine the inductive element, the frequency range of measurement can be continued to the lower ones. Existence of inductive loop in the Nyquist plot feature of stainless steels can be related to the localised corrosion as it reported previously [27–29].

In this study, CPT value of two types of stainless steels including 2205 duplex stainless steel (DSS2205) and 20Cr–28Ni super austenitic stainless steel (20Cr–28Ni) has been measured by potentiodynamic and potentiostatic polarisation. The results are compared by the results of new proposed EIS method.

3. Experimental methods

The chemical composition analysis of alloys in weight percent is illustrated in Table 1. Samples were prepared in rod type to avoid any crevice corrosion during pitting corrosion measurements. The rod specimen had 10 mm diameter and 40 mm length with hemispherical end. Orientation of long axis of rod working electrodes was normal to the rolling direction. The immersion depth of working electrode was 12 mm; therefore, the immersion surface area was $4\ \text{cm}^2$. Samples were abraded up to 1200 emery paper, washed in distilled water and eventually dried by hot air. Saturated calomel electrode (SCE) and platinum wire were used as reference and counter electrodes, respectively and electrochemical tests were conceded by means of ACM instruments automated potentiostat (Gill AC).

The CPT values of both alloys were measured in 0.1 M NaCl solution by potentiodynamic and potentiostatic polarisations. Potentiodynamic polarisation measurement was carried out at temperatures varying from $25\ ^\circ\text{C}$ ($\pm 1\ ^\circ\text{C}$) to temperatures in which pitting corrosion was observed with a $10\ ^\circ\text{C}$ increment to obtain the breakdown potential. Before the measurements, open circuit potential (OCP) was obtained for 60 min. The potentiodynamic measurement rate was $0.5\ \text{mV}\ \text{s}^{-1}$, starting at 50 mV below OCP up to the anodic potential value at which an abrupt increase in current density occurred. The sudden current increase was either due to extensive pitting corrosion or transpassivity dissolution. The potential at which the current density exceeded $100\ \mu\text{A}/\text{cm}^2$ was defined as the breakdown potential (E_b) [30]. To employ potentiostatic polarisation, the specimens were polarised at anodic potential of 600 mV/SCE and temperature was increased by a rate of $0.6\ ^\circ\text{C}/\text{min}$. The CPT value was considered as the temperature which current density reached $100\ \mu\text{A}/\text{cm}^2$ [31]. To employ EIS as a new method, EIS tests were performed in 0.1 M NaCl solution at temperatures varying from $15\ ^\circ\text{C}$ ($\pm 1\ ^\circ\text{C}$) to temperatures in which pitting corrosion was observed with a $10\ ^\circ\text{C}$ increment. A *dc* offset potential of 600 mV/SCE was employed at all the experiments and the magnitude of *ac* potential was 15 mV and the frequency ranges from 10 kHz to 3 Hz. Each experiment was repeated for three times to ensure their reproducibility.

Table 1
Chemical composition of used alloys (wt%).

	C	Cr	Ni	Mo	S	P	Mn	Si	N	Cu	Other	Fe
DSS2205	0.03	21.61	5.31	3.07	0.0007	0.022	0.97	0.74	0.3	–	<0.5	Bal
20Cr–28Ni	0.05	20.46	28.82	5.05	0.009	0.045	1.4	0.55	–	0.22	<0.5	Bal

4. Results and discussion

4.1. Potentiodynamic CPT measurements

Potentiodynamic polarisation curves of DSS2205 and 20Cr–28Ni alloys in 0.1 M NaCl at different temperatures are shown in Fig. 1. Generally, by increasing the temperature from lower temperatures to higher ones, the passivity current density increases. For instance in the case of DSS2205, it increased from 2.6 to 4 $\mu\text{A}/\text{cm}^2$ when temperature increased from 25 to 65 $^{\circ}\text{C}$, respectively. In 20Cr–28Ni alloy, by rising the temperature from 15 to 65 $^{\circ}\text{C}$, the passivity current density (current density corresponding to the 200 mV/SCE) increases continuously from 0.93 to 10 $\mu\text{A}/\text{cm}^2$. Moreover, the breakdown potential (potential associated to 100 $\mu\text{A}/\text{cm}^2$ anodic current density) decreased. The breakdown potential of DSS2205 decreases from 1200 mV/SCE at 25 $^{\circ}\text{C}$ to 500 mV/SCE at 65 $^{\circ}\text{C}$ and this decrease for 20Cr–28Ni alloy was from 1200 mV/SCE at 15 $^{\circ}\text{C}$ to 300 mV/SCE at 65 $^{\circ}\text{C}$. It can be observed that in 0.1 M NaCl, DSS2205 and 20Cr–28Ni show passiv-

ity behaviour in the temperature ranges of 25–45 $^{\circ}\text{C}$ and 15–35 $^{\circ}\text{C}$, respectively. At 55 $^{\circ}\text{C}$, increase of current density fluctuations in passivity domain of DSS2205 is observed and a transition from transpassivity to pitting corrosion is detected; see Fig. 1. This behaviour was observed at 45 $^{\circ}\text{C}$ for 20Cr–28Ni. Based on potential value associated to 100 $\mu\text{A}/\text{cm}^2$, the criterion for the breakdown potential, the pitting potential of ca 970 mV at 55 $^{\circ}\text{C}$ is observed for DSS2205 and it was ca 700 mV at 45 $^{\circ}\text{C}$ for 20Cr–28Ni. Hence the passivity domain of DSS2205 (from OCP to breakdown potential) is decreased from 1300 mV at 45 $^{\circ}\text{C}$ to 690 mV at 65 $^{\circ}\text{C}$ and similar decreases can be observed for 20Cr–28Ni from 1300 mV at 35 $^{\circ}\text{C}$ to 570 mV at 55 $^{\circ}\text{C}$ and 450 mV at 65 $^{\circ}\text{C}$. In summary, based on potentiodynamic measurements in various temperatures, shown in Fig. 2 in DSS2205 alloy, a transition from transpassivity to pitting corrosion occurs between 45 and 55 $^{\circ}\text{C}$ and this transition for 20Cr–28Ni was from 35 to 45 $^{\circ}\text{C}$ in 0.1 M NaCl solution.

4.2. Potentiostatic CPT measurement

Fig. 3, represents the results on assessment of CPT of DSS2205 and 20Cr–28Ni with potentiostatic measurement by applying the 600 mV/SCE anodic potential and increasing in temperature gradually. Considering the 100 $\mu\text{A}/\text{cm}^2$ current density as criteria for CPT evaluation, it can be seen that the CPT of DSS2205 and 20Cr–28Ni were 60 and 55 $^{\circ}\text{C}$ in 0.1 M NaCl.

The potentiostatic results revealed that the current density associated to the applied anodic potential decreases at the beginning of the test. This decrease of current density was due to thickening of the passivating film on the surface. This decrease in current density continued up to almost 40 and 30 $^{\circ}\text{C}$ for DSS2205 and 20Cr–28Ni, respectively. After this potential, the background current density increases gradually. The minimum background current density was 1.25 and 2.4 $\mu\text{A}/\text{cm}^2$ for DSS2205 and 20Cr–28Ni, respectively. This value for passivity current density is significantly higher than that of previously reported for passivity current density of stainless steel [32]. This is because of the shorter time of experiment and also the effect of temperature and surface area.

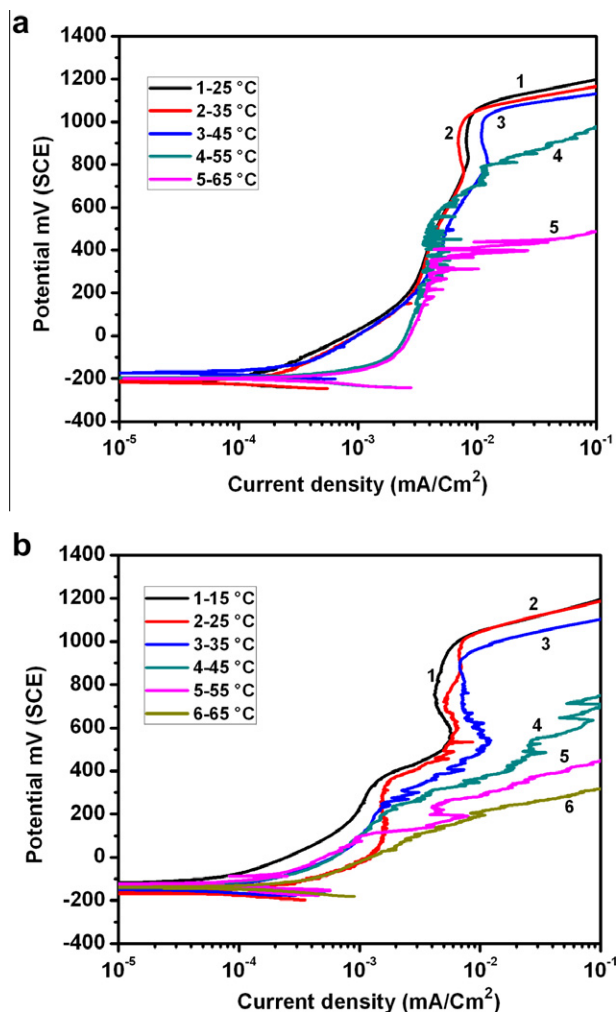


Fig. 1. Potentiodynamic polarisation results of a) DSS2205 and b) 20Cr–28Ni in 0.1 M NaCl solution at different temperatures.

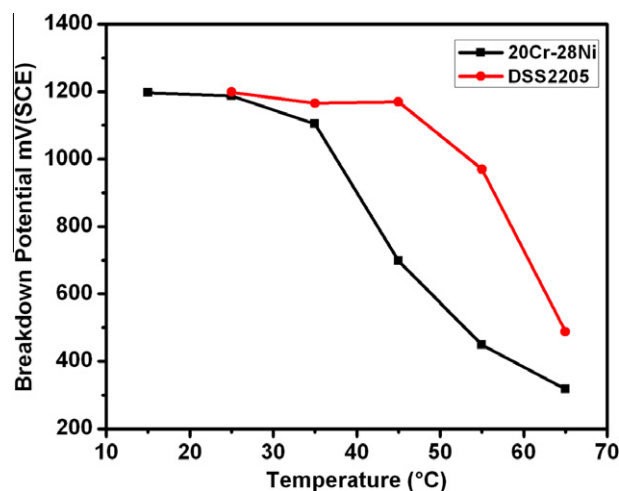


Fig. 2. Breakdown potential vs. temperature for both alloys in 0.1 M NaCl solution at different temperatures.

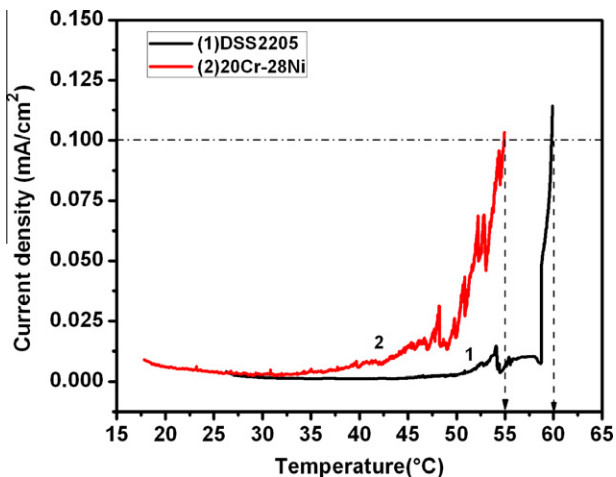


Fig. 3. Potentiostatic polarisation results of DSS2205 and 20Cr-28Ni alloys at 600 mV/SCE in 0.1 M NaCl solution.

By further increase in temperature, at about 47 °C for DSS2205 and 23 °C for 20Cr-28Ni, the metastable pits can be detectable. It is noticeable that the magnitude of current density of metastable pitting occurrence on stainless steels is too much lower than the background current density in this study [32]. In fact, the metastable pitting occurs at lower temperature and since their magnitude is lower than that of passivity background current density, they cannot be detected. At the temperatures higher than 47 °C for DSS2205 and 23 °C for 20Cr-28Ni, the magnitude of these metastable pitting occurrence were higher than background current density therefore they become detectable. Further increase in temperature increase the magnitude of the metastable pits current density and they tend to become stable. According to the CPT determining model, proposed by Laycock et al [6], the CPT is the temperature in which the critical current density within the pit becomes higher than limiting current density due to salt film precipitation within the pit. In fact, by rising the temperature both limiting current density and critical current density increases. While, the pit current density of metastable pit is lower than limiting current density due to salt precipitation, the metastable pit is repassivated. This shows itself as an individual metastable pitting occurrence in potentiostatic results in which after an increase in current density, it suddenly decreases to the passivity current density. It means the pit solution chemistry is not high enough concentrated of metal cations for salt film precipitation. When the pit current density becomes higher than that of limiting current density, the pit propagates continuously and becomes stable. This shows itself as a continuous increase in current density of potentiostatic results, revealing stable pitting occurrence.

By looking to the presented results of potentiostatic and potentiodynamic polarisation methods, it is clear that there is about 10–15 °C difference between the results of potentiostatic polarisation and potentiodynamic polarisation for both alloys. This is because of the difference between the origins of these two types of CPT measurement methods. In the case of potentiostatic measurements, an applied anodic potential in passivity domain of alloy produces an integrated passivity on the entire surface and this passivity was modified by further increase in temperature below the CPT of alloy. Hence, the breakdown of thicker passivity occurs at higher temperatures.

4.3. CPT measurement by EIS method

Fig. 4 shows the EIS results of DSS2205 and 20Cr-28Ni in 0.1 M NaCl solution at applied anodic potential of 600 mV/SCE in the

frequency range of 10000–3 Hz. Fig. 4 shows that by rising the temperature, the diameter of depressed semi circle decreases. The equivalent circuits which are used for modelling the EIS results are shown in Fig. 5 and the extracted parameters according to the model is presented in Table 2. As it can be seen, at lower temperatures, the Nyquist plots contain only a simple randel-like feature which is attributed to the passive surface. In these models constant phase element (CPE) is used for more accurately analysing of impedance behaviour of the electric double layer. The impedance of the CPE is expressed as [33]:

$$Z_{CPE} = P^{-1} (i\omega)^{-n} \tag{1}$$

where P is the magnitude of the CPE; ω the angular frequency; n as the deviation parameter ($0.5 \leq n \leq 1$ which is dependent on the surface morphology).

For a circuit including a CPE, the double layer capacitance (C_{dl}) can be calculated from CPE parameter values P and n using the following expression [34].

$$C_{dl} = P^{1/n} R_{ct}^{1-n/n} \tag{2}$$

At the temperatures above the CPT in which stable pits are formed on the surface, the equivalent circuit defers with that of lower temperatures as it was shown in Fig. 5. In these circuits there is three more element due to stable pits on the surface named as

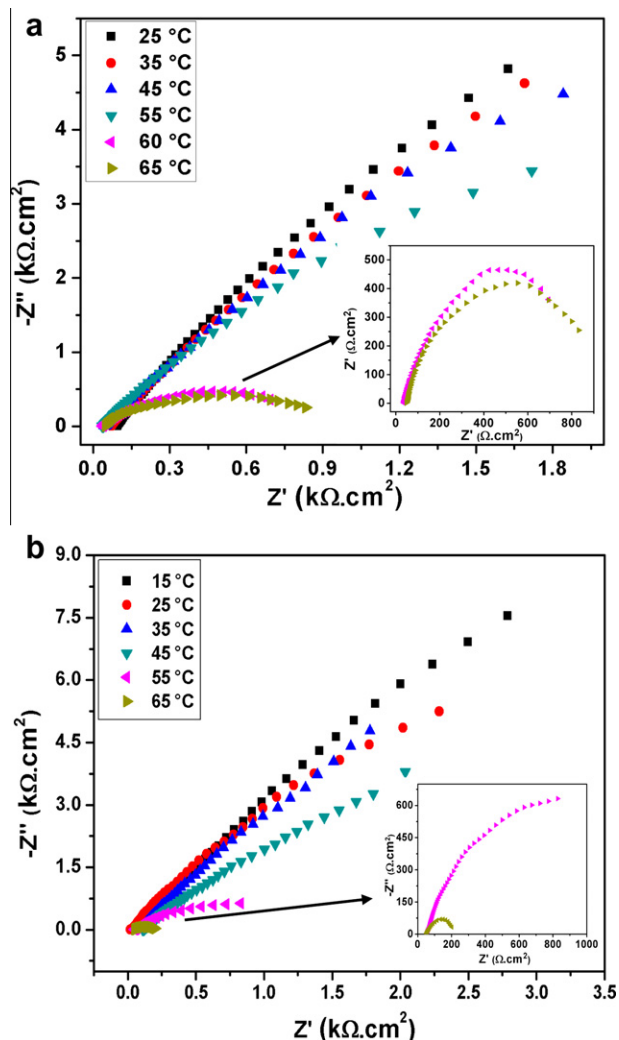


Fig. 4. EIS result of a) DSS2205 and b) 20Cr-28Ni at different temperatures and applied anodic dc potential of 600 mV/SCE.

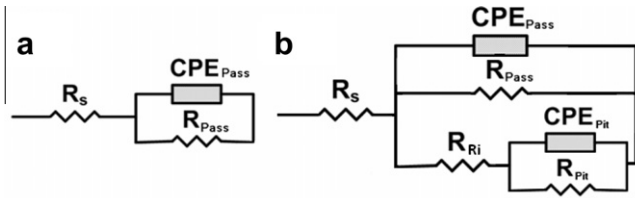


Fig. 5. Equivalent circuits which are used for modelling the EIS results a) below CPT and b) above CPT.

CPE_{pit}, R_{pit} and R_i which are the double layer formed at interface between surface and solution in pit, charge transfer resistance related to pit and the pit solution resistance, respectively.

Fig. 6 shows the proposed equivalent circuit of the surface prior (Fig 6a) and after stable pit formation (Fig. 6b). When stable pits are formed, the surface is separated in two distinguishable parts i.e. passive surface and pitted area. At the passive surface, the proposed circuit is similar to the lower temperatures. However, at the presence of stable pit on the surface, a new physical element (stable pit) which is parallel to the passive surface is added. Two stable pit resistances, pit charge transfer resistance (R_{pit}), and pit solution resistance (R_i), are defined (Fig 6b). At this circumstance, for calculation of the pit double layer capacitance, the value of pit charge transfer resistance, R_{pit}, using Eq. (2) is used.

As it can be seen from Table 2 for both materials at all temperatures, by rising the temperature, charge transfer resistance decreases, P-value increases and n-value also decreases. For temperatures below CPT, the decrease in R_{pass} may be attributed to the increase in ions diffusion through the passive layer which indicates

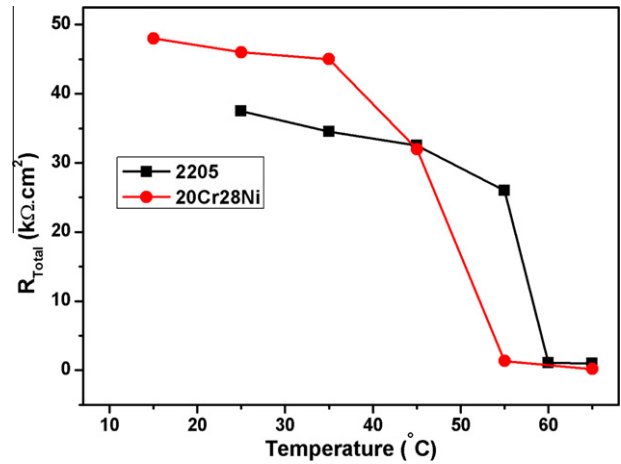


Fig. 7. Variation of total resistance (R_{total}) values vs. temperature for DSS2205 and 20Cr-28Ni.

increasing the defects on the passive film. In addition, decrease of n-value shows the destructive effect of temperature on the homogeneity of passive layer. In addition, while there is no stable pit on the surface, the capacitance of double layer has increased.

Considering the Helmholtz model of the surface film capacitance, it is defined that the capacitance is inversely proportional to the surface film thickness [33,35]:

$$C_{dl} = \frac{\epsilon^0 \epsilon S}{d} \tag{3}$$

Table 2
Obtained results of EIS method at 600 mV/SCE, for DSS2205 and 20Cr-28Ni alloys in 0.1 M NaCl solution at different temperatures.

Type of steel	T (°C)	R _{pass} (Ω cm ²)	R _{pit} (Ω cm ²)	R _i (Ω cm ²)	CPE _{pass} parameters		CPE _{pass} (μF/cm ²)	CPE _{pit} parameter		CPE _{pit} (μF/cm ²)
					P (μF/cm ²)	n		P (μF/cm ²)	n	
DSS2205	25	37500	–	–	38.9	0.88	40.96	–	–	–
	35	34500	–	–	40.7	0.87	42.82	–	–	–
	45	32500	–	–	41.7	0.86	43.82	–	–	–
	55	26000	–	–	50.4	0.83	53.27	–	–	–
	60	20650	740	370	38.0	0.93	37.31	20.1	0.92	13.94
20Cr-28Ni	65	19850	685	350	29.7	0.90	28.01	18.0	0.89	10.46
	15	48000	–	–	23.2	0.90	23.48	–	–	–
	25	46000	–	–	36.0	0.84	39.63	–	–	–
	35	45000	–	–	45.0	0.84	51.47	–	–	–
	45	32000	–	–	54.0	0.79	62.45	–	–	–
	55	24000	920	500	39.8	0.89	39.58	37.5	0.82	17.91
	65	22000	80	85	28.2	0.90	26.74	19.6	0.99	18.36

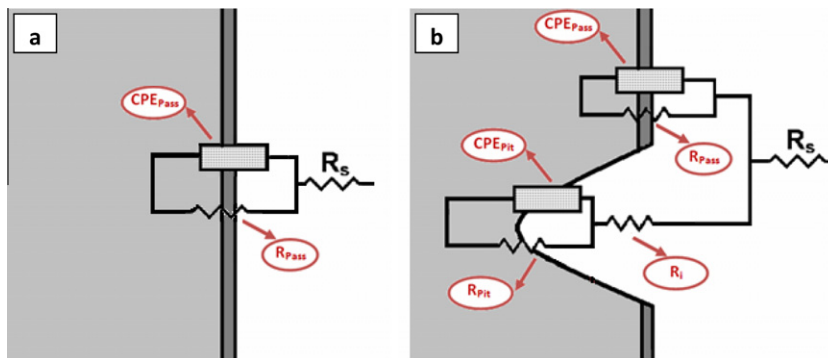


Fig. 6. Proposed model for the equivalent circuit on the surface a) below CPT b) above CPT.

where d is the thickness of the film, S is the surface of the electrode, ϵ^0 is the permittivity of the air, and ϵ is the local dielectric constant. This increase in double layer capacitance of passive layer below CPT is attributed to the decrease in double layer thickness due to the increase of passive layer defects.

As it was mentioned above, the CPT can be considered as the temperature in which there is a sharp decrease in R_{total} . At temperature lower than the CPT, the value of R_{total} is equal to R_{pass} . Whereas at temperatures above the CPT, R_{total} is calculated by the following equation

$$R_{\text{total}} = \frac{(R_{\text{pit}} + R_i) \cdot R_{\text{pass}}}{(R_{\text{pit}} + R_i + R_{\text{pass}})} \quad (4)$$

Fig. 7 shows the change in the R_{total} values (calculated from the data in Table 2) vs. temperature for both investigated alloys. As it can be seen, for DSS2205, this sharp decrease occurred at temperature between 55 and 60 °C. The decrease in breakdown potential for 20Cr–28Ni begins at 45 °C and then continues to decrease sharply to 55 °C. It is proposed that the CPT value for 20Cr–28Ni lies between 45 and 55 °C. Considering other results of other techniques i.e. potentiostatic and potentiodynamic polarisation methods, it can be seen that the results obtained by EIS method show close correlation with results of other two techniques. These comparable results show that the EIS can be suitably used as the method of determination of CPT of stainless steels. In addition, since this method is used at high frequencies (10000–3 Hz), it is a fast method for CPT determination. Additionally, unlike the potentiostatic polarisation method in which passive layer was modified at lower temperatures, in this method, at the temperatures above the CPT, the alloy was immediately subjected to the pitting condition. As a consequence, the CPT results of the EIS method can be considered as more reliable results. In fact, as it mentioned in Section 2, there are two ways for subjecting the alloy to higher potentials than its normal corrosion potential in neutral environment. One of them was polarisation with the additional dc potential and the other one is choosing an oxidising solution (e.g. 10% FeCl₃). In this new method, the additional dc potential was used. The reason of using this additional potential was to immediately subjecting the alloy to pitting condition.

5. Conclusions

In this study a new method for determination of CPT of stainless steels based on EIS method has been proposed and the following results were obtained:

1. The measured CPT value of DSS2205 and 20Cr–28Ni by potentiodynamic polarisation method were at temperature between 45–55 °C and 35–45 °C, respectively and potentiostatic polarisation method gives values of 60 and 55 °C for CPT of DSS2205 and 20Cr–28Ni, respectively.
2. The EIS method can be used as an alternating method for measuring the CPT of stainless steels. At the temperatures in which pitting corrosion occurs, the charge transfer resistance decreases significantly.
3. The CPT value of DSS2205 and 20Cr–28Ni measured by EIS method is between 55–60 °C and 45–55 °C, respectively which are close to the values determined by the two previous methods specially potentiostatic ones.
4. EIS results revealed that the double layer capacitance in temperatures below the CPT increases by increasing the temperature. This increase in double layer capacitance is attributed to the decrease in double layer thickness due to the increase of passive layer defects.

Acknowledgements

Authors would like to appreciate the financial support from Ferdowsi University of Mashhad provision of laboratory facilities during the period that this research was conducted. Authors would also like to acknowledge Dr. James J. Noël for his final grammatical correction of the paper.

References

- [1] R.J. Brigham, E.W. Tozer, Temperature as a pitting criterion, *Corrosion* 29 (1973) 33–36.
- [2] R.J. Brigham, E.W. Tozer, Effect of alloying additions on the pitting resistance of 18% Cr austenitic stainless steel, *Corrosion* 30 (1974) 161–166.
- [3] R.J. Brigham, Pitting of Mo bearing austenitic stainless steel, *Corrosion* 28 (1972) 177–179.
- [4] R.J. Brigham, Effect of Cr on the pitting resistance of austenitic stainless steels, *Corros. Sci.* 15 (1975) 579–580.
- [5] R.J. Brigham, E.W. Tozer, Pitting resistance of 18% Cr ferritic stainless steels containing molybdenum, *J. Electrochem. Soc.* 121 (1974) 1192–1193.
- [6] N.J. Laycock, M.H. Moayed, R.C. Newman, Metastable pitting and the critical pitting temperature, *J. Electrochem. Soc.* 145 (1998) 2622–2628.
- [7] R. Ovarfort, New electrochemical cell for pitting corrosion testing, *Corros. Sci.* 28 (1988) 135–137, 139–140.
- [8] R. Ovarfort, Critical pitting temperature measurements of stainless steels with an improved electrochemical method, *Corros. Sci.* 29 (1989) 987–993.
- [9] P.E. Arnvig, A.D. Bisgard, Determining the potential independent critical pitting temperature (CPT) by potentiostatic method using the Avesta cell, in: *Proceeding of the Conference on Corrosion 96*, NACE, Houston, TX, 1996, paper 437.
- [10] ASTM G48 – Standard Test Methods for Pitting and Crevice Corrosion Resistance of Stainless Steels and Related Alloys by Use of Chloride Solution, West Conshohocken, USA, 2003.
- [11] L.F. Garfias-Mesias, J.M. Sykes, C.D.S. Tuck, The effect of phase compositions on the pitting corrosion of 25 Cr duplex stainless steel in chloride solutions, *Corros. Sci.* 38 (1996) 1319–1330.
- [12] V.M. Salinas-Bravo, R.C. Newman, An alternative method to determine critical pitting temperature of stainless steels in ferric chloride solution, *Corros. Sci.* 36 (1994) 67–77.
- [13] P.L. Guevel, N. Jallerat, J.C. Bavay, K.V. Quang, Critical Pitting Temperature of Stainless Steels determined by a fast method, *Corrosion Control Conference*, (1987).
- [14] K. Vu Quang, P. Le Guevel, N. Jallerat, J.C. Bavay, Fast method for determination of critical pitting temperature, *Corros. Sci.* 28 (1988) 423–424.
- [15] M.G.S. Ferreira, J.L. Dawson, Electrochemical studies of the passive film on 316 stainless steel in chloride media, *J. Electrochem. Soc.* 132 (1985) 760–765.
- [16] J. Hitzig, K. Juttner, W.J. Lorenz, W. Paatsch, AC-impedance measurements on corroded porous aluminum oxide films, *J. Electrochem. Soc.* 133 (1986) 887–892.
- [17] H.S. Isaacs, M.W. Kendig, Determination of surface inhomogeneities using a scanning probe impedance technique, *Corrosion* 36 (1980) 269–274.
- [18] M. Keddad, R. Oltra, J.C. Colson, A. Desestret, Depassivation of iron by straining and by abrasion: an A.C. impedance study, *Corros. Sci.* 23 (1983) 441–451.
- [19] F. Mansfeld, S. Lin, K. Kim, H. Shih, Pitting and surface modification of SiC/Al, *Corros. Sci.* 27 (1987) 997–1000.
- [20] R. Oltra, M. Keddad, Application of impedance technique to localized corrosion, *Corros. Sci.* 28 (1–5) (1988) 7–18.
- [21] J.R. Park, D.D. Macdonald, Impedance studies of the growth of porous magnetite films on carbon steel in high temperature aqueous systems, *Corros. Sci.* 23 (1983) 295–315.
- [22] R. Oltra, M. Keddad, Application of EIS to localized corrosion, *Electrochim. Acta* 35 (1990) 1619–1629.
- [23] N. Ebrahimi, M.H. Moayed, A. Davoodi, Critical pitting temperature dependence of 2205 duplex stainless steel on dichromate ion concentration in chloride medium, *Corros. Sci.* 53 (2011) 1278–1287.
- [24] L. Bai, B.E. Conway, Three-dimensional impedance spectroscopy diagrams for processes involving electroadsorbed intermediates, introducing the third electrode-potential variable—examination of conditions leading to pseudo-inductive behavior, *Electrochim. Acta* 38 (1993) 1803–1815.
- [25] K. Darowicki, The fixed state in impedance measurements of a two-step electrode reaction proceeding with accompanying adsorption of an intermediate product, *Electrochim. Acta* 42 (1997) 1073–1079.
- [26] M.M.J. Pieterse, M. Sluyters-Rehbach, J.H. Sluyters, A faradaic impedance study of the reduction of oxygen from aqueous alkaline solution at the dropping mercury electrode, *J. Electroanal. Chem. Interfacial Electrochem.* 107 (1980) 247–256.
- [27] A. Arutunow, K. Darowicki, DEIS assessment of AISI 304 stainless steel dissolution process in conditions of intergranular corrosion, *Electrochim. Acta* 53 (2008) 4387–4395.
- [28] A. Arutunow, K. Darowicki, DEIS evaluation of the relative effective surface area of AISI 304 stainless steel dissolution process in conditions of intergranular corrosion, *Electrochim. Acta* 54 (2009) 1034–1041.

- [29] P. de Lima-Neto, J.P. Farias, L.F.G. Herculano, H.C. de Miranda, W.S. Araújo, J.-B. Jorcin, N. Pébère, Determination of the sensitized zone extension in welded AISI 304 stainless steel using non-destructive electrochemical techniques, *Corros. Sci.* 50 (2008) 1149–1155.
- [30] A. Igual Muñoz, J. García Antón, J.L. Guiñón, V. Pérez Herranz, Inhibition effect of chromate on the passivation and pitting corrosion of a duplex stainless steel in LiBr solutions using electrochemical techniques, *Corros. Sci.* 49 (2007) 3200–3225.
- [31] C.J. Semino, J.R. Galvele, Passivity breakdown of high purity iron and AISI 4340 steel in 0.5 M NaCl solution, *Corros. Sci.* 16 (1976) 297–300.
- [32] G.T. Burstein, B.T. Daymond, The remarkable passivity of austenitic stainless steel in sulphuric acid solution and the effect of repetitive temperature cycling, *Corros. Sci.* 51 (2009) 2249–2252.
- [33] N.S. Ayati, S. Khandandel, M. Momeni, M.H. Moayed, A. Davoodi, M. Rahimizadeh, Inhibitive effect of synthesized 2-(3-pyridyl)-3,4-dihydro-4-quinazolinone as a corrosion inhibitor for mild steel in hydrochloric acid, *Mater. Chem. Phys.* 126 (2011) 873–879.
- [34] B. Hirschorn, M.E. Orazem, B. Tribollet, V. Vivier, I. Frateur, M. Musiani, Determination of effective capacitance and film thickness from constant-phase-element parameters, *Electrochim. Acta* 55 (2010) 6218–6227.
- [35] A. Kosari, M. Momeni, R. Parvizi, M. Zakeri, M.H. Moayed, A. Davoodi, H. Eshghi, Theoretical and electrochemical assessment of inhibitive behavior of some thiophenol derivatives on mild steel in HCl, *Corros. Sci.* 53 (2011) 3058–3067.